OCTOBER 25 2024

Assessing impact of near-ground meteorology on spectral variability in static jet aircraft noise measurements FREE

Jacob B. Streeter; Tyce W. Olaveson; Matthew A. Christian; Kent L. Gee ; Alan T. Wall; Steven C. Campbell

Proc. Mtgs. Acoust. 50, 040010 (2022)
https://doi.org/10.1121/2.0001969

Volume 50 http://acousticalsociety.org/

183rd Meeting of the Acoustical Society of America
Nashville, Tennessee
5-9 December 2022

Noise: Paper 4pNS4

Assessing impact of near-ground meteorology on spectral variability in static jet aircraft noise measurements

Jacob B. Streeter
Brigham Young University, Provo, UT; jacobbstreeter@gmail.com

Tyce W. Olaveson, Matthew A. Christian and Kent L. Gee
Department of Physics and Astronomy, Brigham Young University, Provo, UT, 84602; tyceolaveson@gmail.com; mattachristian66@gmail.com; kentgee@byu.edu

Alan T. Wall
Air Force Research Laboratory, Wright-Patterson AFB, OH; alan.wall.4@us.af.mil

Steven C. Campbell
Ball Aerospace and Technologies Corp., Beavercreek, OH; steven.campbell.28.ctr@us.af.mil

ANSI/ASA standard S12.75 (2012) provides guidance on allowable meteorological conditions for acoustical measurements of installed high-performance jet engines. This paper investigates meteorological effects on acquired acoustical data by analyzing recent measurements of a T-7A-installed GE F404 engine. During this measurement, the aircraft was run up six times at engine powers from idle to full afterburner, with test conditions following those prescribed by S12.75. However, far-field spectra are surprisingly variable, despite a morning measurement with low wind conditions. Analysis of the vertical temperature gradient shows a correlation between the gradient and spectral characteristics at distances as short as 38 m from the aircraft. The results suggest that local temperature profiles must be considered more carefully in future full-scale measurements and the results studied to establish guidelines for inclusion in the standard.

Published by the Acoustical Society of America

https://doi.org/10.1121/2.0001969.

1. INTRODUCTION

Noise radiation from high-performance military jets poses hearing-loss risk to those near the aircraft, most notably launch personnel on aircraft carriers, and adversely affects communities near military bases. To address these issues, the Department of Defense has put significant resources towards developing jet noise reduction technology (Martens et al., 2010). Investigations tend to come in three classes: numerical simulations, lab-scale experiments, and full-scale measurements (Wall et al., 2022). Each provides insights into the noise problem and in the end, changes how full-scale jets operate. To accurately gauge the impact of new nozzle designs, full-scale military aircraft must have a consistent measurement procedure.

The current standard for ground-based measurements is given by ANSI/ASA S12.75, which outlines the measurement requirements, including descriptions of measuring meteorological conditions, microphone placement, and data analysis. It states that acquiring "Accurate, reliable, and repeatable noise measures from standardized noise measurement techniques will help ensure confidence in the data used in the modeling and prediction of noise impacts" (ANSI S12.75-2012). In recent years, these standards have been applied to full-scale measurements of an F-35 (James et al., 2015) and the T-7A "Red Hawk" (Leete et al., 2021). Studies from BYU have used these data sets in jet noise source characterizations (e.g., Harker et al. 2019; Mathews et al. 2024) and radiation studies (e.g., Leete et al. 2018; Olaveson et al. 2024).

In the T-7A data analyses, spectral inconsistencies across engine run-ups have required that the analysis not use the entire dataset. This paper discusses these spectral inconsistencies and explores the various external factors outlined by ANSI S12.75 that may impact the individual measurements. While the measurement conditions fall within the specified standards, the presence of a variable temperature gradient appears to impact noise propagation for specific runs. We recommend the standard be updated to include bounds on the vertical temperature gradient.

2. T-7A MEASUREMENT

In the early morning on August 18th, 2019, at Holloman Air Force Base, New Mexico, acoustic data were collected from the T-7A "Red Hawk" trainer aircraft. The aircraft was equipped with a GE-F404 afterburning capable turbofan engine. The aircraft was strapped to the runway and oriented facing the blast deflector to preserve the jet structure as much as possible (see Fig. 1). The experiment featured six run-ups where the engine was cycled through each engine condition, namely idle, 75% N2, 88% N2, 88% N2, full military power (MIL), and afterburner (AB). Each condition was held steady long enough to collect 30 seconds of data before moving on to the next condition.

The acoustical measurement featured over 200 microphones, capturing both the near and far-field radiation. Near-field imaging arrays included several linear arrays used for source characterization and noise impact on launch personnel (see ANSI S12.75). Far-field arrays were placed in concentric arcs between 18m (63 ft) and 229 m (750 ft). Each was centered on the microphone array reference point (MARP) located 13 ft downstream of the nozzle exit, which approximates the maximum radiation region. Figure 2 shows three far-field arrays relative to the aircraft. In addition to the acoustic measurements, three weather stations were placed at 2ft, 5ft, and 20 ft above the ground to capture meteorological data including temperature, pressure, and humidity. These stations, shown in Fig. 2 as red triangles, were placed along a line perpendicular to the centerline at 180 ft downstream and at 185 ft, 195 ft, and 215 ft respectively, with the 20 ft station being the farthest away. Since the stations are relatively far away from the aircraft, it is expected that heat from the jet will have a negligible impact on the local environment. A complete overview of the measurement can be found in Leete et al. (2021).

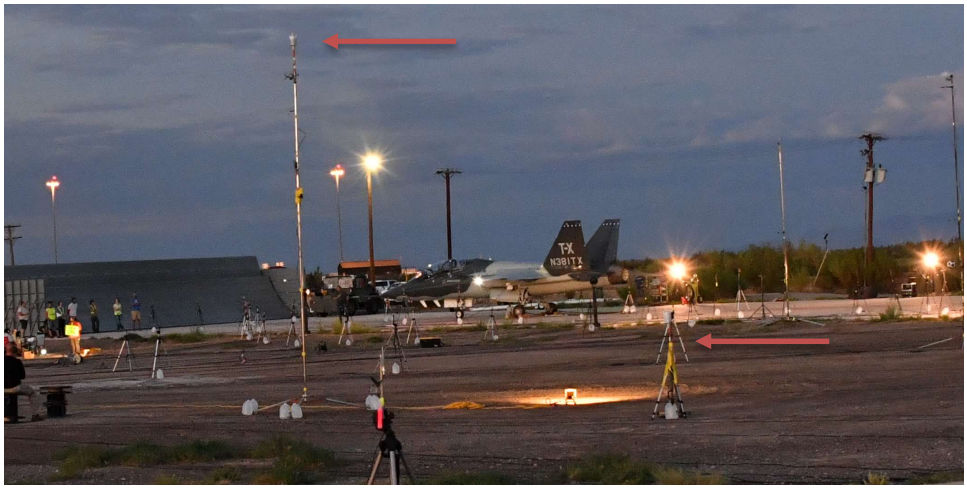

Figure 1. T-7A measurement setup. Two weather stations (indicated with orange arrows) are seen in the foreground. The third is out of frame to the right.

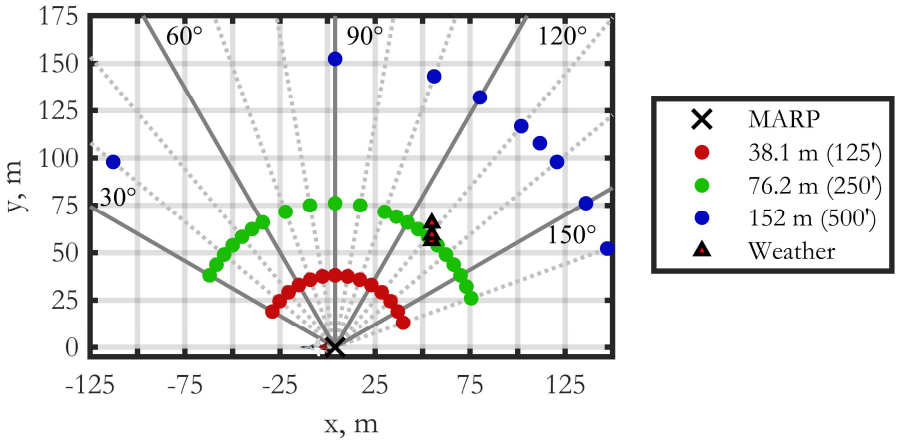

Figure 2. T-7A measurement array layout. Weather stations are shown as red triangles near the green 250' arc.

3. RESULTS AND ANALYSIS

This section discusses significant variation in far-field spectra and reviews the various weather parameters that might be contributing.

A. T-7A SPECTRAL ANALYSIS

For each of the 125', 250' and 500' far-field arcs, autospectra are created using the full 30 sec measurement and a frequency bin width of 3 Hz. Figure 3 shows the autospectral densities of each run for AB (left) and MIL (right) at 90°. Figure 4 is the same as Fig. 3 but zoomed in on the main spectral peak to highlight the differences between runs. Due to the elevated microphones, each spectrum features a strong interference null near 800 Hz. Christian et al. (2023) have implemented a model for addressing the ground reflections in analysis, but one concern that remains is the spectral location of the nulls across runs. For runs 1 and 2 at AB, the interference nulls shift to lower frequencies. The differences are most apparent at the nearest arcs, though other discrepancies creep in with distance. At 500', runs 5 and 6 are significantly different from runs 3 and 4, which are in turn different from runs 1 and 2. The same behavior is observed at MIL. Since the measurement configuration remained constant during the entire experiment, variations between runs are due to changes in either the aircraft operating conditions or the ambient environment. The remainder of this section explores these possibilities.

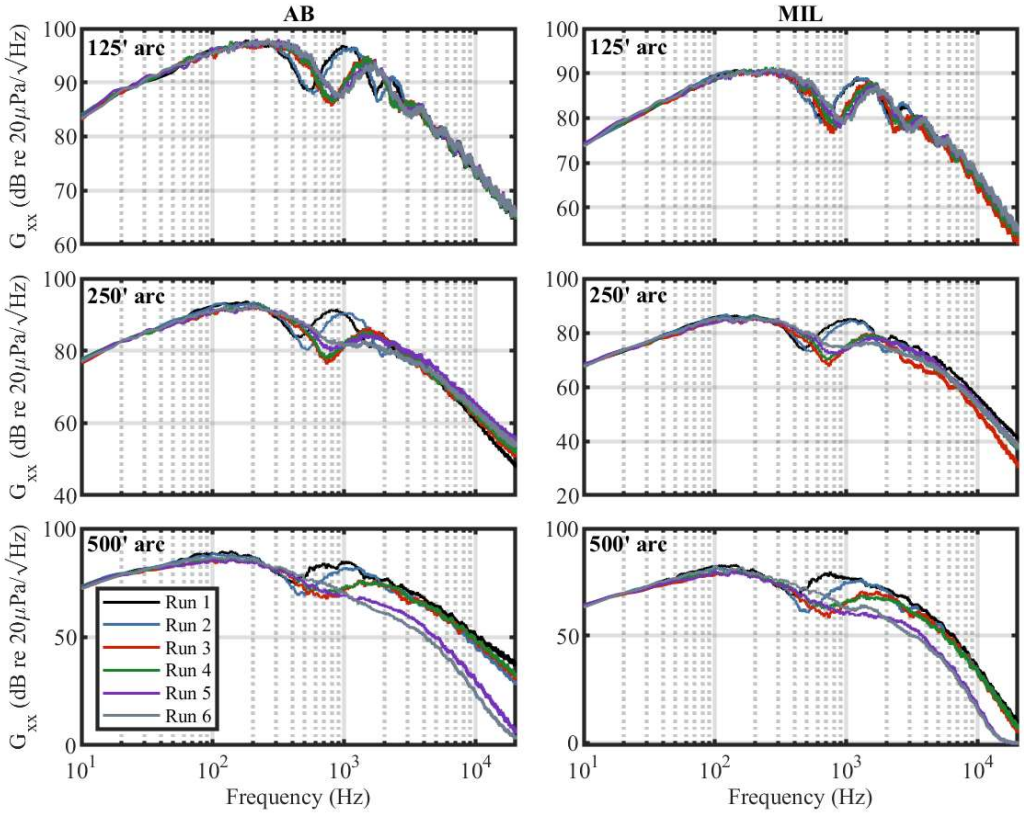

Figure 3. Autospectral densities (G_{xx}) for AB (left) and MIL (right) at 90° for three far-field arcs. At 125' and 250', the spectral maxima and minima differ from runs 3-6. At 500', the data are variable across all six runs.

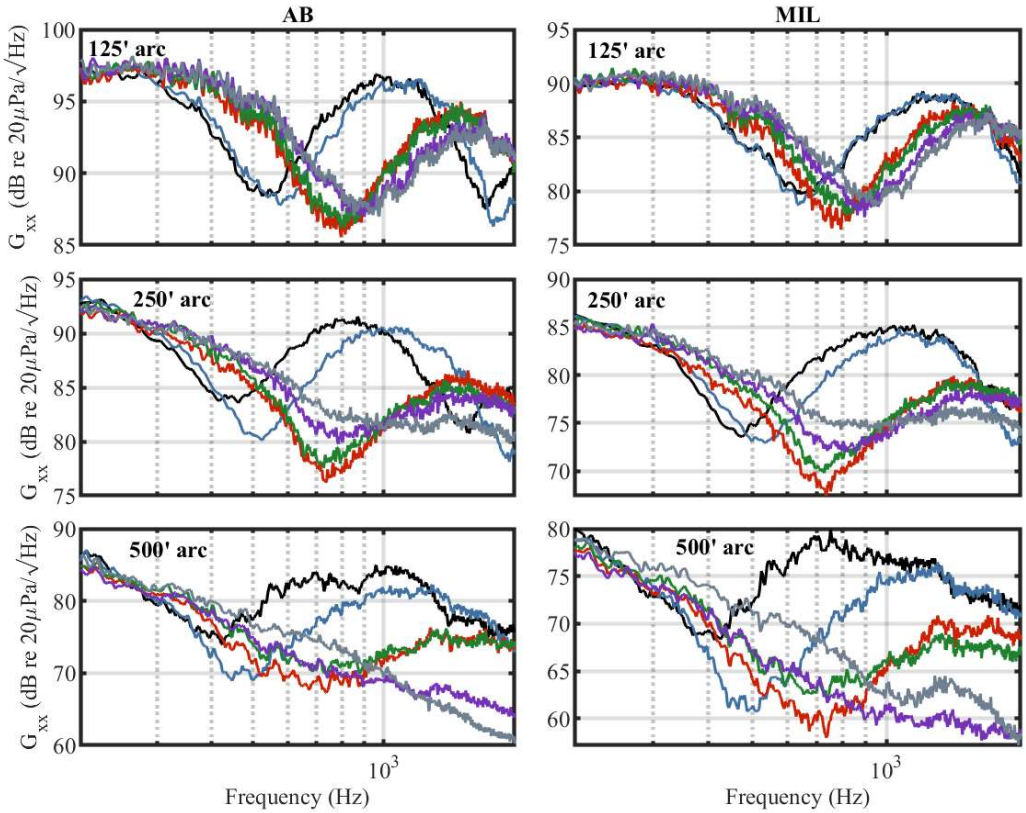

Figure 4. Same as Fig. 3, but zoomed in on the spectral peak to demonstrate the spectral discrepancies

During the experiment, the aircraft thrust (engine condition) was manually adjusted by the pilot. The operating thrust is directly correlated with the pilot lever angle (PLA). Figure 5 shows the PLA as a function of local time (in HH:MM) for the entire duration of the measurement. Six "tower" structures are seen within the figure, indicating the time and duration of each of the six run-ups. Each step on the tower shows where the thrust was increased to the next engine condition. Horizontal, red, dashed lines show the nominal PLA for each of the measured engine conditions. Trenches between blocks are where the aircraft was powered down between each set of run-ups. Thrust variations between each run-up are observed as deviations from the red line. While there is more difference for the lower engine powers, the spectra in Fig. 3 are for MIL and AB conditions where there are insignificant deviations from the expected PLA. At MIL and AB, changes of 1° in PLA result in less than a 0.5% difference to the gross thrust. Since the deviations in PLA are less than this, there is negligible change in thrust between run-ups for MIL and AB.

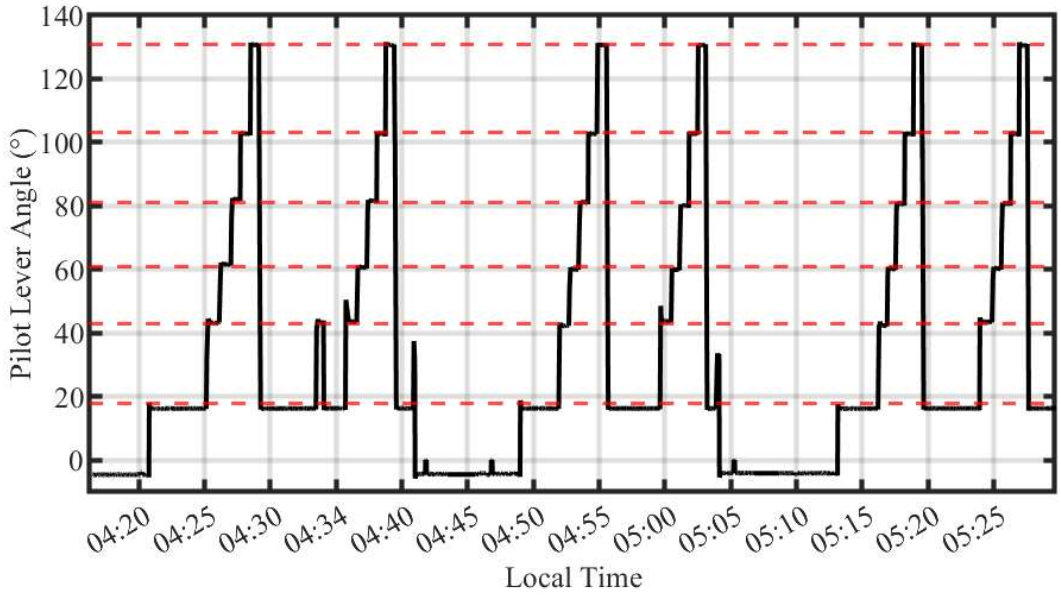

Figure 5. Pilot lever angle time series. Vertical jumps show where the aircraft changed engine powers.

B. WEATHER

The ANSI standard has guidelines for acceptable weather conditions to improve data fidelity and maintain consistency between experiments. During the T-7A measurement, ambient conditions were recorded by three weather stations at 2ft, 5ft, and 20 ft above the ground, as described in Section 2. This section considers the effects of wind, pressure, humidity, and temperature as they relate to the ANSI standard, and their potential impact on the far-field spectra.

For wind, the standard says: "The surface wind conditions (5 feet AGL) shall not exceed 8 knots maximum with 5-knot maximum cross-winds" (ANSI S12.75-2012). Table 1 shows the wind speed (in knots) and the wind direction averaged across each of the three weather stations. Differences between the individual stations were minimal. While the wind direction varied from run to run, the average wind speed remained well within standards. At 125' and 250', runs 1 and 2 feature the strongest spectral shifts (see Fig 3); however, they share relatively little in terms of wind speed and direction. Moreover, similar wind speeds between runs 1 and 3 do not appear to correlate with spectral deformations. Also note that runs 2 and 6 have identical wind directions, yet their spectra are quite different.

Table 1. Average wind speed and direction collected from the three weather stations. Individual differences between stations are minimal.

	Run 1	Run 2	Run 3	Run 4	Run 5	Run 6
Average Wind Speed (Knots)	2.40	1.79	2.12	2.89	2.88	3.39
Average Wind Direction	139°	11°	19°	321°	346°	11°

The next parameter is ambient pressure. The ANSI standard does not provide any hard guidelines for measuring atmospheric pressure beyond simply recording it. Figure 6 shows the recorded ambient pressure at two weather stations in inches of mercury (in-Hg). Note that no data was collected at the third station due to hardware error. Over the course of the entire measurement, the pressure fluctuated no more than 0.01 in-Hg, which is close to the instrument precision. Relative to the rest of the measurement, this is a minimal change. Even if a significant change were present, the microphones used in this experiment were ported, which would remove the impact of a variable atmospheric pressure at these time scales.

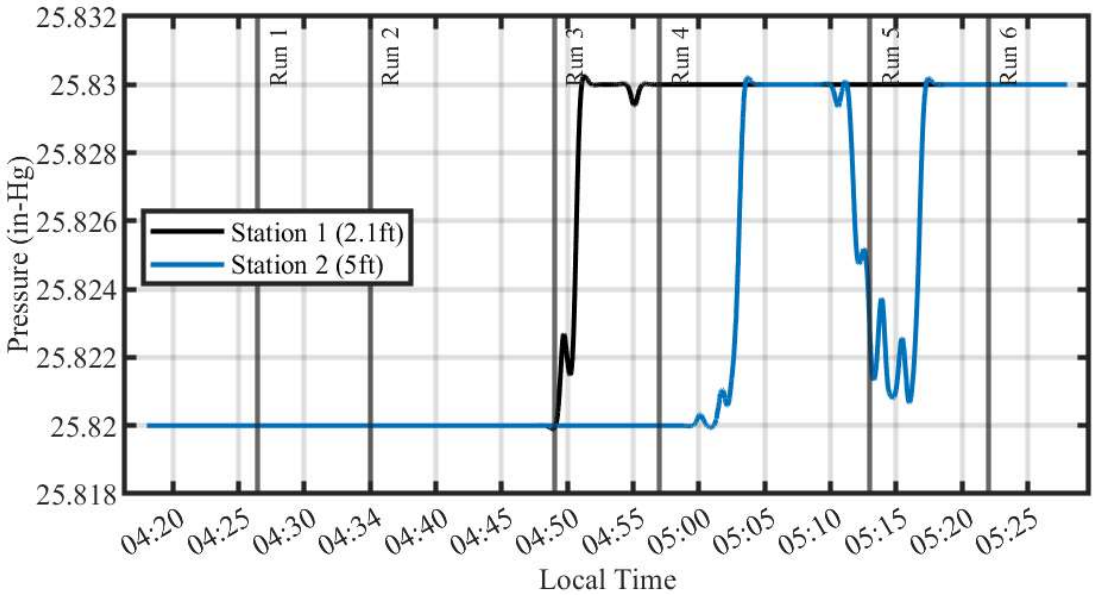

Figure 6. Ambient pressure during the measurement

Next is the relative humidity. The ANSI standard states: “The relative humidity [must be] greater than 20 percent…and no more than 90 percent”. (ANSI S12.75-2012). Figure 7 shows the time series collected from each of the three weather stations. During the entire measurement, the relative humidity remains within the standard. The most prominent feature is the large difference between station 3 and the others between runs 1 and 2. This difference gradually collapses as the measurement continues. Since relative humidity is a function of the ambient temperature, similar trends are seen in the temperature plot of Fig. 8.

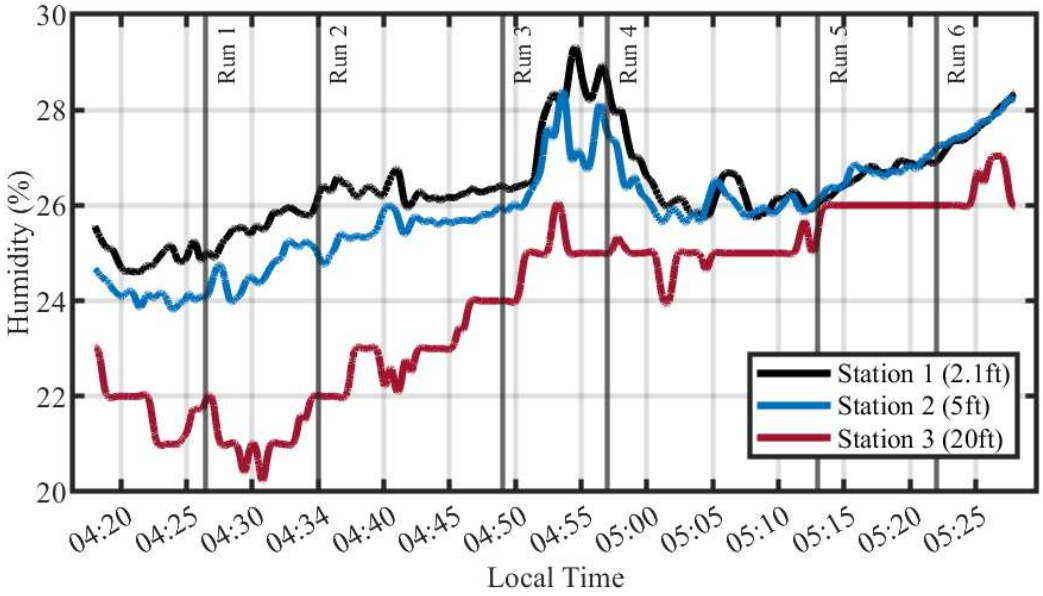

Figure 7. Ambient relative humidity

The final weather parameter is the temperature. The ANSI standard states that the temperature "shall be no less than 36°F and shall be no more than 95°F". Figure 8 shows the temperature as measured by each of the three stations. The temperature variation is well within standards. As with relative humidity, there is a significant difference between station 3 and the others during the time interval between runs 1 and 2. This difference gradually collapses throughout the measurement. While humidity has a strong impact on frequency-dependent atmospheric absorption, near-ground temperature variations can have a strong impact on noise radiation (Embleton et al., 1976). The red curve in Figure 8 comes from a station that is physically higher than the others, thus this difference indicates the presence of a temperature gradient during the first two runs. Since the sound speed is dependent on temperature, a gradient in temperature will result in a sound speed gradient. When a sound wave propagates through a medium with varying sound speeds, the wave naturally refracts toward the lowest sound speed. In the case of the T-7A measurement, the temperature gradient in the early run-ups could result in upward noise refracting through the atmosphere down onto the measurement setup. This path length increase would result in a lower interference null, which is observed in the spectra for runs 1 and 2 relative to the others. Another prominent feature in Fig. 8 is the temperature inversion that occurs just before run 5. While the effects of a temperature inversion are not thoroughly studied here, it is possible that the strong spectral disagreement between runs 5 and 6 at 500' is related to this atmosphere. Further research is needed.

While the standard mentions temperature gradients, there is no guideline beyond simply measuring it. Since it is suspected that the temperature gradient has impacted at least a few runs of the T-7A measurement, it is recommended that further investigation be done on the impact of temperature gradients and temperature inversions and appropriate guidelines be developed. This will be important for maintaining consistency between measurements.

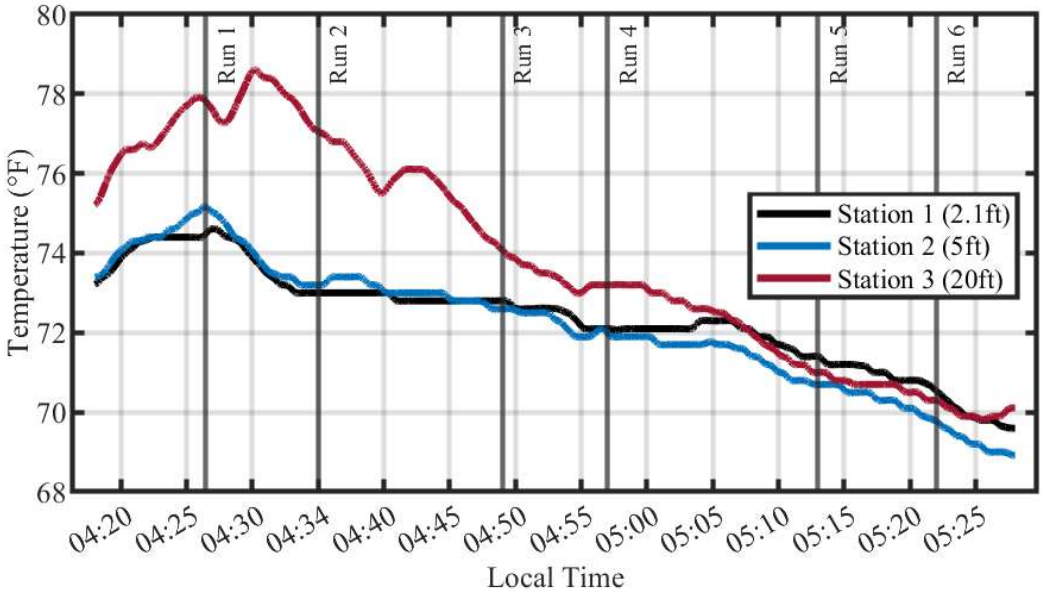

Figure 8. Ambient temperature at three stations during the T-7A run-up.

The spectral variations seen in this paper are not unique to the T-7A measurement. Gee et al. (2022) notes the presence of a temperature gradient during a measurement of an F-35 adhering to the same ANSI standard. Their measurement featured a more extensive set of far-field arcs with microphones placed as far as 1220 m (4000'). The spectra for individual runs become increasingly varied with distance, similar to the T-7A spectra at 500', though the problem becomes more exaggerated with distance. Beyond the far-field spectral messiness, an F-35 nonlinear propagation analysis performed by Reichman et al. (2016) showed spectra at 305 m (1000') that had spectral nulls that were not consistent with simple ground reflection interactions.

4. CONCLUSION

This paper has reported on meteorological data collected near a T-7A trainer aircraft during an acoustical measurement. These data were collected in compliance with the standards outlined in ANSI S12.75. Despite the strict adherence to these standards, significant spectral differences between runs 1 and 2 at 125' and 250' relative to runs 3-6 suggest a factor that is unaccounted for in the standard. The measured wind, pressure, humidity, and temperature revealed the presence of a strong temperature gradient during the early hours of the experiment. The potential impact of a temperature gradient on spectral data underscores the need for further investigation and a potential revision of the measurement standard.

ACKNOWLEDGMENTS

This work is funded by the Office of Naval Research grant number N00014-21-1-2069, titled "Connecting Analyses of Installed Tactical Jet Engine Noise with Simulated and Laboratory-Scale Data," with project monitor Dr. Steven Martens (Code 351 Jet Noise Reduction).

REFERENCES

ANSI/ASA, "Methods for the Measurement of Noise Emissions from High Performance Military Jet Aircraft,", ANSI/ASA S12.75-2012.

Christian, M. A., Gee, K. L., Streeter, J. B., Wall, A. T., and Campbell, S. C., "Sound power and acoustic efficiency of an installed GE F404 jet engine," *JASA Express Lett* 3, 073601, 2023. https://doi.org/10.1121/10.0019866

Embleton, T. F. W., Thiessen, G. J., and Piercy, J. E., "Propagation in an inversion and reflections at the ground," *The Journal of the Acoustical Society of America*, **59**, 278-282, 1976. https://doi.org/10.1121/1.380883

Gee, K. L., Reichman, B. O., and Wall, A. T., "Effects of meteorology on long-range nonlinear propagation of jet noise from a static, high-performance military aircraft," *Proc. Mtgs. Acoust.* 35, 040006, 2018. https://doi.org/10.1121/2.0001531

Harker, B. M., Gee, K. L., Neilsen, T. B., Wall, A. T., and James, M. M., "Source characterization of full-scale tactical jet noise from phased-array measurements," *The Journal of the Acoustical Society of America*, **146**, 665, 2019. https://doi.org/10.1121/1.5118239

James, M. M., Salton, A. R., Downing, J. M., Gee, K. L., Neilsen, T. B., Reichman, B. O., McKinely, R. L., Wall, A. T., and Gallagher, H. L., "Acoustic Emissions from F-35 Aircraft during Ground Run-Up," *21st AIAA/CEAS Aeroacoustics Conference*, 23-26 June 2015, Dallas, TX. https://doi.org/10.2514/6.2015-2375

Leete, K. M., Wall, A. T., Gee, K. L., Neilsen, T. B., James, M. M., and Downing, J. M., "Acoustical Holography-Based Analysis of Spatiospectral Lobes in High-Performance Aircraft Jet Noise," *AIAA J.*, Vol. 59, No. 10, 2018. https://doi.org/10.2514/1.J059400

Leete, K. M., Vaugh, A. B., Bassett, M. S., Rasband, R. D., Novakovich, D. J., Gee, K. L., Campbell, S. C., Mobley, F. S., and Wall, A. T., "Jet Noise Measurements of an Installed GE F404 Engine," *AIAA Scitech 2021 Forum*, 11-15, 19-21 January 2021, Virtual Event. https://doi.org/10.2514/6.2021-1638

Mathews, L. T. and Gee, K. L., "Acoustical Holography and Coherence-Based Noise Source Characterization of an Installed F404 Engine," *AIAA Journal*, Vol 62, No. 6, June 2024. https://doi.org/10.2514/1.J063543

Martens, S. and Spyropoulos, J. T., "Practical Jet Noise Reduction for Tactical Aircraft," *Proceedings of ASME Turbo Expo 2010: Power for Land, Sea and Air,* June 14-18, 2010, Glasgow, UK. https://doi.org/10.1115/GT2010-23699

Olaveson, T. W. and Gee, K. L., "Wavelet-Based Characterization of Spatiospectrotemporal Structures in F404 Engine Jet Noise," *AIAA J.* 2024, Article in Advance. https://doi.org/10.2514/1.J063944

Reichman, B., Wall, A. T., Gee, K. L., Neilsen, T. B., Downing, J. M., James, M. M., and McKinley, R. L. "Modeling Far-field Acoustical NOnlinearty from F-35 Aircraft during Ground Run-up," *54th AIAA Aerospace Sciences Meeting*, San Diego, CA, January 2016, AIAA Paper No 2016-1888. https://doi.org/10.2514/6.2016-1888

Wall, A. T., Gee, K. L., Morris, P. J., Colonius, T., and Lowe, K. T., "Introduction to the special issue on supersonic jet noise," *The Journal of the Acoustical Society of America*, **151**, 806, 2022. https://doi.org/10.1121/10.0009321